Measuring the Probability Density of Quantum Confined States

P. H. Beton, J. Wang, N. Mori, L. Eaves, P. C. Main, T. J. Foster, and M. Henini
Department of Physics, University of Nottingham, Nottingham NG7 2RD, United Kingdom
(Received 12 January 1995)

We show that it is possible to measure the probability density of a quantum-confined state using resonant magnetotunneling. We have measured the probability densities of the lowest three bound states formed in a semiconductor nanostructure and show that they are eigenstates of a parabolic potential.

PACS numbers: 73.40.Gk, 73.40.Kp, 73.50.Jt

The solution to Schrödinger's equation for a given potential consists of a set of energy eignvalues and corresponding eigenfunctions, or wave functions. Generally eigenvalues may be measured using spectroscopic techniques, but direct measurement of wave functions is usually not possible. Recently it has been demonstrated that it is possible to measure the wave functions of quantum-confined states formed in nanostructures formed on metallic surfaces [1,2]. In these experiments a scanning tunneling microscope (STM) was used both to fabricate the nanostructure and to probe the wave functions of the bound states. Interestingly, Crommie, Lutz, and Eigler [1] argue that while the wave functions of bound states formed in STM nanostructures may be measured, this is not possible for conventional semiconductor nanostructures.

In this Letter we show that, contrary to this view, it is possible to measure the wave functions of quantum-confined states formed in a semiconductor heterostructure. This is achieved by resonant magnetotunneling between 1D quantum-confined states. We have recently shown [3] that the energy eigenvalues of these states may be measured using resonant magnetotunneling. In this paper we show that for an even smaller device in which the lateral quantization is much stronger, it is also possible to measure the probability density of the corresponding eigenfunctions. Experimentally we measure the magnetic field dependence of the tunnel current between an initial and a final quantum-confined state. From this dependence we may deduce the Fourier transform of the final state wave function. In particular, we have measured the probability density of the lowest three bound states of a parabolic potential. These wave functions are well known theoretically and used widely in physics; however, it has not previously been possible to measure them directly. Our technique is complementary to the STM work in that we use a magnetic field (rather than spatial control) to vary the overlap between initial and final states, and also we are able to probe electronic states below the surface of a structure.

Our experimental device is a resonant tunneling diode with submicron lateral dimensions. Figure 1 is a schematic diagram showing the device parameters and an outline of the principles of operation. The device is fabricated using optical lithography and selective wet etching from a GaAs/AlAs heterostucture grown by molecular beam epitaxy. Full details of sample fabrication may be found in Wang *et al.* [4]. The GaAs quantum well has

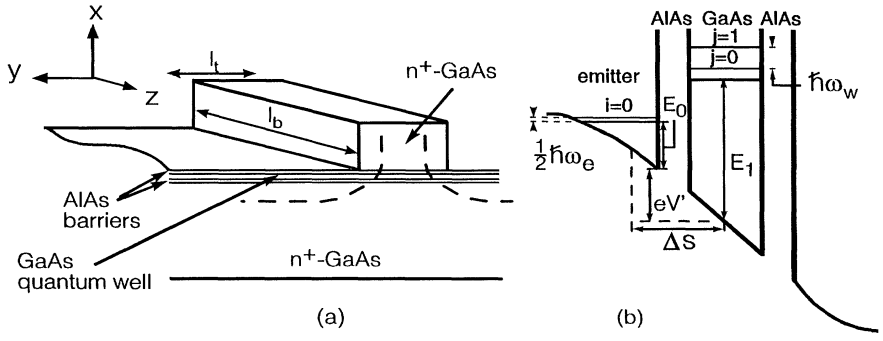

FIG. 1. (a) A schematic diagram of the active region of our device. The top n^+ GaAs is etched into the shape of a bar with dimensions $l_t \times l_b$. Depletion due to surface effects extends up to the dotted line. (b) Conduction band profile of the device under an applied bias. A quasibound state is formed in the quantum well with confinement energy E_1 (= 40 meV for our device). For the doping profile used in our device, an accumulation layer is formed at the emitter barrier under an applied bias which has a confinement energy E_0. The energy of the ith state in the emitter is thus $E_0 + (i + 1/2)\hbar\omega_e/2$ and of the jth state in the well is $E_1 + (j + 1/2)\hbar\omega_w$. Resonant tunneling via the jth state in the well is possible when V is adjusted (V' depends linearly on V) so that it is aligned in energy with the $i = 0$ state in the emitter.

 0031-9007/95/75(10)/1996(4)$06.00

width $w = 9.0$ nm and is formed between two AlAs tunnel barriers of width $b = 4.7$ nm. Si-doped n-type GaAs contact layers are formed on either side of the barriers. Sidewall depletion due to pinning of the free surfaces at midgap extends up to the dotted line [see Fig. 1(a)]. The physical dimensions $l_t \times l_b = 0.5 \times 1.0\ \mu m^2$, but the electrically conducting area is much smaller due to sidewall depletion; we estimate $50 \times 600\ nm^2$.

The two AlAs tunnel barriers produce conventional quantum well confinement along x. Under applied bias electrons are also confined along x in the approximately triangular potential well of the emitter accumulation layer. Because of the submicron lateral dimensions, the motion of electrons in the y direction is also quantized. A set of i ($i = 0, 1, 2, \ldots$) one-dimensional subbands is formed in the emitter, and j ($j = 0, 1, 2, \ldots$) one-dimensional subbands in the well. We take the confining potential along y to be parabolic, which we show below is an excellent approximation. The energy separation of the 1D subbands in the emitter and well is given by $\hbar\omega_e$ and $\hbar\omega_w$, respectively, and the wave functions of the ith and jth subbands by $\varphi_i^e(y)$ and $\varphi_j^w(y)$.

Figure 2 shows the low temperature ($T = 0.3$ K) $I(V)$ for this device in the presence of a magnetic field, B, oriented along z. For $B = 0$ T we observe additional peaks (as compared with the large area diode—see inset to Fig. 2) due to resonant tunneling via different 1D subbands formed in the quantum well. Note that the resonances in the small area diode occur at higher voltages than for the large area diode. This is an electrostatic effect that has been discussed previously [5]. As B is progressively increased, the peak labeled $j = 0$ decreases in amplitude, whereas that labeled $j = 2$ first decreases, then increases, and is finally reduced to zero. Between these two peaks a third peak appears which is absent at $B = 0$ T. This is labeled $j = 1$ and is observed clearly in the range $2 < B < 7$ T, but then disappears as B is further increased. At higher field a series of regularly spaced peaks is observed in $I(V)$ identified by arrows in Fig. 2. In addition we observe a number of weaker peaks in our data, including a sharp rise in current at the onset for resonant tunneling ($V = 1.31$ V).

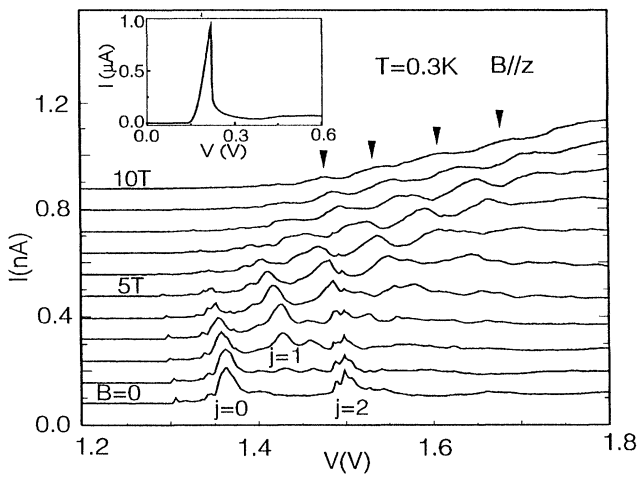

FIG. 2. $I(V)$ characteristics of a submicron resonant tunneling diode in the presence of a magnetic field parallel to z. Lowest curve is for $B = 0$ T; top curve is for $B = 10$ T in 1 T steps. Inset shows $I(V)$ ($B = 0$ T) for a large area diode fabricated from the same semiconductor heterostructure. Additional peaks in $I(V)$ are observed in the submicron diode, as compared with the large area device.

In our device the lower contact has a larger conducting width than either the quantum well or the top contact (see Fig. 1). For the polarity shown in Fig. 2, electrons flow to the top contact so that $\hbar\omega_e < \hbar\omega_w$.

For this device at low temperature almost all the electrons in the emitter occupy the lowest ($i = 0$) state. This is a key difference as compared with our previous work on a larger device in which many subbands were occupied in the emitter and the resulting $I(V)$ was a convolution of resonances from all occupied states [3]. We show below that it is possible to extract the probability density of the laterally confined states in the quantum well if only one emitter state is occupied.

Resonant tunneling via the jth state occurs when the voltage is adjusted so that the lowest state in the emitter is aligned in energy with the jth state in the well, i.e., $eV' + E_0 + \hbar\omega_e/2 = E_1 + (j + 1/2)\hbar\omega_w$. The current flowing through state j, $I_j(B)$, is proportional to the modulus squared of the matrix element between the initial and final states, $M_j(B)$, given by (Mori *et al.* [6], Demmerle *et al.* [7], and Wang *et al.* [3])

$$M_j(B) = \int_{-\infty}^{\infty} dy\ \exp\{-ik_0 y\}\varphi_0^e(y)\varphi_j^w(y) = \int_{-\infty}^{\infty} dk_y \Phi_0^e(k_y - k_0)\Phi_j^w(k_y), \quad (1)$$

where $\phi_0^e(k_y) = \int_{-\infty}^{\infty} \varphi(y)\exp(ik_y y)\,dy$ and $\Phi_j^w(k_y)$ are the Fourier transforms of the emitter and well wave functions. The magnetic field dependence enters through the parameter $k_0 = eB\Delta s/\hbar$, where Δs is the separation of the emitter and well states in the x direction (we estimate $\Delta s = 20$ nm). Equation (1) is derived from a quantum mechanical treatment. However, the quantity k_0 may be related to the classical change in kinetic momentum of an electron moving in a magnetic field. Classically such an electron executes a curved orbit, and in moving a distance Δs in the x direction changes its kinetic momentum in the y direction by $eB\Delta s(= \hbar k_0)$. In a quantum mechanical formulation for a large area diode, the effect of the magnetic field is to introduce a wave-vector shift equal to k_0 [8–10] in the initial and final states (which are plane waves). For a small area diode, k_0 enters as a wave-vector shift between the Fourier transforms of the initial and final confined state wave functions.

We can account for the principal peaks in our data as follows—the peaks labeled 0 and 2 arise from resonant tunneling from the $i = 0$ (symmetric) state in the emitter into state j (= 0 and 2) in the well. Tunneling via the antisymmetric state $j = 1$ is strongly forbidden by parity conservation at $B = 0$, since the matrix element defined in Eq. (1) is zero for this case. However, this restriction is relaxed for $B > 0$, and the peak labeled 1 in Fig. 2 is due to tunneling via the $j = 1$ level.

From Eq. (1) we see that the application of a magnetic field provides a means of measuring the probability density of the confined states formed in the quantum well with a resolution in k space given by the width of the Fourier transform of the emitter wave function. In the limit $\hbar\omega_w \gg \hbar\omega_e$, when the emitter states have a narrow spread (i.e., a small half-width) in k_y, the peak current through the jth state $I_j \sim |\phi_j(k_0)|^2$. Figure 3 shows the $j = 0$, 1, and 2 peak currents plotted versus magnetic field together with the theoretical probability densities of simple harmonic oscillator (SHO) states. There is excellent agreement between our data and the theoretical plots if the value of k_w [$= (m\omega_w/\hbar)^{1/2}$, the natural wave vector scale for SHO states] is chosen so that the theoretical and experimental maxima for the $j = 1$ state coincide. This choice corresponds to $\hbar\omega_w = 10$ meV, and a characteristic length scale for the wave function, $k_w^{-1} = 10$ nm. The width of the initial state $[\Phi_0^e(k_y) = (\pi k_e^2)^{-1/4} \exp(-k_y^2/2k_e^2)$, where $k_e = (m\omega_e/\hbar)^{1/2}]$ limits the resolution of the minimum of the $j = 2$ state. In addition, the $j = 0$ state is broadened from $I_j(B) \propto \exp(-k_0^2/k_w^2)$ (the result expected for an infinitely narrow initial state)

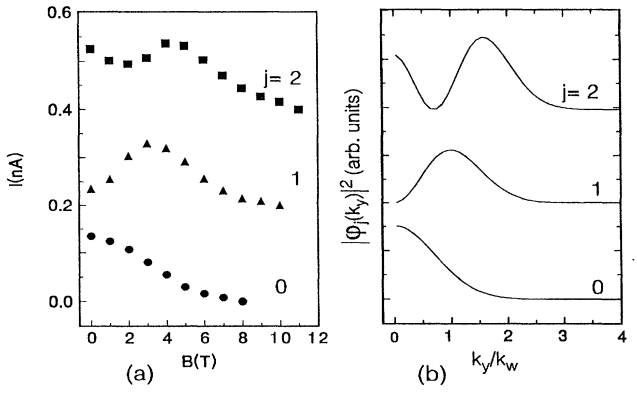

FIG. 3. (a) Variation of peak currents with magnetic field for the $j = 0$, 1, and 2 (circles, triangles, and squares, respectively) peaks. The experimental data are displaced for clarity. (b) $|\Phi_j(k_y)|^2$ the probability densities for the $j = 0$, 1, and 2 simple harmonic oscillator states. $k_w = [= (m\omega_w/\hbar)^{1/2}]$ is the natural wave vector for a SHO state. The maximum for the $j = 1$ state occurs at $k_y/k_w \approx 1$ and experimentally at $B \approx 3.1$ T corresponding to a value of $k_0 = eB\Delta s/\hbar \approx 9.1 \times 10^7$ m^{-1}. Equating this value with k_w gives $\hbar\omega_w = 10$ meV.

to $I_j(B) \propto \exp(-k_0^2/(k_w^2 + k_e^2))$. From a comparison of our data with theoretical curves, we estimate that $\hbar\omega_e = 5$ meV. Note that $\hbar\omega_e \approx \hbar\omega_w/2$ is consistent with our previous measurements on larger devices in which several subbands are occupied in the emitter [3]. The voltage separation of the $j = 0$ and $j = 2$ is approximately 140 mV. These states are separated by 20 meV in energy which gives a leverage ratio, $k = 7$. This falls within the range of values ($k = 6$–8.5) which we have previously reported for these devices [3].

The series of peaks in $I(V)$ observed at higher voltage and high magnetic field (see Fig. 2) is due to resonant tunneling via states with higher index ($j > 2$). For these states we are able to resolve only the largest peak in $|\Phi_j(k_y)|^2$ which occurs near the classical turning point, $k_{j,\max} \approx [2m(j + 1/2)\hbar\omega_w]^{1/2}/\hbar$. Note also from Eq. (2) that for all states $I_j(B) \to 0$ in the limit $k_0 > k_{j,\max}$, in agreement with our data.

So far we have discussed only the effects of tunneling from the $i = 0$ state. From measurements on the same device taken for B oriented parallel to y, we have established that there is a marginal occupation of the $i = 1$ state in the emitter, i.e., the Fermi energy in the emitter, $E_F, \sim 3\hbar\omega_e/2$. Tunneling from this state gives rise to a number of weak peaks in $I(V)$; for example, the peak which occurs at $V = 1.4$ V for $B = 0$ T in Fig. 2 corresponds to tunneling from $i = 1$ via $j = 1$. Although this is interesting, the $i = 1$ wave function has a more complex form than for $i = 0$, and therefore we are unable to extract the final state wave function from the magnetic field dependence of these peaks.

Finally we remark that our explanation assumes that electrons are independent. It is possible that some of the other weaker peaks in our data are due to electron-electron interactions. In particular, the sharp peak that is observed at the onset for conduction is highly reminiscent of a Fermi edge singularity which we have recently reported [11].

We have shown that it is possible to measure the probability density of quantum-confined states formed in semiconductor nanostructures using resonant magnetotunneling. The application of a magnetic field induces a relative shift in momentum space between the initial and final states between which electrons tunnel. For the case considered here, the confining potential is close to parabolic; however, it is clear from the above analysis that the technique can in principle be applied to electrons confined in potential wells of arbitrary shape.

This work was funded in part by EPSRC and in part by ESPRIT Basic Research Action 'PARTNERS'. L. E. thanks the EPSRC for financial support and N. M. thanks the British Council.

[1] M. F. Crommie, C. P. Lutz, and D. Eigler, Nature (London) **363**, 524–527 (1993); Science **262**, 218 (1993).

[2] Y. Hasegawa and Ph. Avouris, Phys. Rev. Lett. **71**, 1071–1074 (1993).

[3] J. Wang, P. H. Beton, N. Mori, L. Eaves, H. Buhmann, L. Mansouri, P. C. Main, T. J. Foster, and M. Henini, Phys. Rev. Lett. **73**, 1146 (1994).

[4] J. Wang, P. H. Beton, N. Mori, H. Buhmann, L. Mansori, L. Eaves, P. C. Main, T. J. Foster, and M. Henini, Appl. Phys. Lett. **65**, 1124 (1994).

[5] M. A. Reed, J. N. Randall, R. J. Aggarwal, R. J. Matyi, T. M. Moore, and A. E. Wetsel, Phys. Rev. Lett. **60**, 535–538 (1988); see also, Reed *et al.*, *Science and Engineering of One and Zero Dimensional Semiconductors*, edited by S. P. Beaumont and C. M. Sotomayer-Torres, NATO ASI Series B (Plenum, New York, 1990), Vol. 214, pp. 139–154.

[6] N. Mori, P. H. Beton, J. Wang, and L. Eaves, Phys. Rev. B **51**, 1735 (1995).

[7] W. Demmerle, J. Smoliner, E. Gornik, G. Bohm, and G. Weimann, Phys. Rev. B **47**, 13 574 (1993).

[8] M. L. Leadbeater, L. Eaves, P. E. Simmonds, G. A. Toombs, F. W. Sheard, P. A. Claxton, G. Hill, and M. A. Pate, Solid State Electron. **31**, 707–710 (1988).

[9] J. Smoliner, W. Demmerle, G. Berthold, E. Gornik, G. Weimann, and W. Schlapp, Phys. Rev. Lett. **63**, 2116–2119 (1989).

[10] R. K. Hayden, D. K. Maude, L. Eaves, E. C. Valadares, M. Henini, F. W. Sheard, O. H. Hughes, J. C. Portal, and L. Cury, Phys. Rev. Lett. **66**, 1749–1753 (1991).

[11] A. K. Geim, P. C. Main, N. La Scala, Jr., L. Eaves, T. J. Foster, P. H. Beton, J.-W. Sakai, F. W. Sheard, M. Henini, G. Hill, and M. A. Pate, Phys. Rev. Lett. **72**, 2061–2064 (1994).